Hot Compaction of Polyoxymethylene. II. Structural Characterization

K. Al Jebawi, B. Sixou, R. Séguéla,* G. Vigier

Groupe d'Etudes de Métallurgie Physique et de Physique des Matériaux, INSA de Lyon, Bâtiment Blaise Pascal, 69621 Villeurbanne, France

Received 22 August 2005; accepted 17 August 2006
DOI 10.1002/app.25400
Published online 29 June 2007 in Wiley InterScience (www.interscience.wiley.com).

ABSTRACT: The structural characterization of sintered polyoxymethylene was carried out to determine the mechanism of sintering. Thermal behavior and small-angle X-ray scattering (SAXS) of sintered samples reveal that an improvement in either crystal size or perfection, or both, takes place during the sintering process, in comparison with compression-molding from the melt. The loss modulus data also give evidence of crystal reorganization during sintering that improves the continuity of the crystalline phase and enhances its mechanical contribution. These findings eliminate the occurrence of major melting during sintering. However, the high mobility of the chains in the crystalline phase in the temperature range of the melting onset suggests that short range rearrangements of the chains in the crystalline lamellae are likely to occur during the time of the process. The proposed mechanism of sintering is that of crystallographic welding of crystals from neighboring particles, as a result of the combined effect of plastic flow and temperature during the hot compaction operation. © 2007 Wiley Periodicals, Inc. J Appl Polym Sci 106: 757–764, 2007

Key words: polyoxymethylene; compaction; sintering; melting behavior; crystal size; molecular mobility; particle welding; powder welding

INTRODUCTION

Polyoxymethylene (POM) is a semi-crystalline thermoplastic polymer with valuable mechanical properties, such as high stiffness, hardness, fatigue, and creep resistance, in conjunction with low friction and wear resistance. These properties make POM particularly suited for manufacturing fixture gears, fan and pump propellers, bearing liners and rings, gear wheels, and pinions. However, POM suffers from a significant shrinkage of injection-molded parts and a natural trend for thermal decomposition with respect to the melting temperature. Sintering of POM powders below the melting temperature appeared as a convenient means for avoiding these drawbacks.

Sintering has been successfully applied in the case of glassy polymers with high glass transition temperature,[1,2] as well as semi-crystalline polymers having very high viscosity above the melting temperature, such as polytetrafluoroethylene[1–3] or ultra-high-molar-weight polyethylene.[4,5]

In a previous paper, we reported on the sintering of POM powders and on the evaluation of the resulting mechanical properties of the sintered parts in comparison with melt-cast materials.[6] Sintered pieces from both native powders and powders grounded from melt-extruded pellets exhibit much higher crystallinity and modulus than their compression-molded counterpart. In addition, the two kinds of sintered materials displayed a significant increase of crystallinity with respect to their corresponding powders.

Although cutter-milling and drilling could be carried out easily, the sintered pieces displayed a typical brittle behavior, i.e., rupture always occurred in the linear elastic domain, whatever the deformation mode.[6] In the case of compressive testing, the material obtained from the sintering of the native powder broke in a brittle mode at 135 MPa, without any sign of anelastic phenomena. In comparison, the compression-molded material displayed an elastic limit at 60 MPa, and a plastic flow stress at 90 MPa. This was a serious hint for efficient welding of the powder particles in the sintered material. Another conclusion was that the crystallites in the sintered material were unable to activate plastic processes. Scanning electron micrographs (SEMs) from the fracture surfaces of the sintered pieces revealed predominant intergranular rupture. However, a number of powder particles displayed intergranular rupture, corroborating efficient welding of the particle and the intrinsic brittleness of the crystallites of the sintered material.

*Present address: Laboratoire Structure et Propriétés de l'État Solide, Université de Lille1, Bâtiment C6, 59655 Villeneuve d'Ascq, France.

Correspondence to: R. Séguéla (roland.seguela@univ-lille1.fr).

Journal of Applied Polymer Science, Vol. 106, 757–764 (2007)

All these findings were taken as evidence that an important reorganization occurred in the crystalline phase during sintering. Particle welding was suggested to result from to the compression-induced shear of the particles in combination with the activation of molecular diffusion in the crystalline phase and at the interface between neighboring crystallites.

The present study deals with the structural characterization of the materials in order to elucidate the mechanism of sintering. Thermal analysis, dynamic mechanical testing, and small-angle X-ray scattering (SAXS) are used to characterize the crystalline phase reorganization during the process.

EXPERIMENTAL

Materials

The materials under investigation are described in Table I. Two kinds of powders provided by Du Pont de Nemours (Geneva, Switzerland) have been used for the sintering process. The native powder, POM-N, consists of fairly spherical particles of average diameter 100 ± 20 μm. The powder ground from melt-extruded pellets, POM-G, has particles of aspect ratio of about 2 : 1 and average length 200 ± 20 μm. The materials sintered from the two powders are labeled POM-NS and POM-GS, respectively.

Methods

Processing of powders into bulk pieces has been carried out by hot compacting under pressure, below the peak melting temperature. The whole hot compaction operation is described in details in the previous work.[6] The temperature was 170°C, the pressure was 25 MPa. The overall procedure consisted of 45 min of thermal conditioning, 30 min of compacting operation, and 15 min of cooling. The final sintered pieces were 10-mm-thick discs of diameter 60 mm. Samples for mechanical experiments were machined out from the discs using a milling cutter. Melt-cast samples were also prepared in the form of 3-mm-thick sheets by compression-molding from the melt at 220°C, and subsequently cooled down to room temperature at ~ 20°C/min, for comparison with the sintered materials.

Differential scanning calorimetry (DSC) was carried out on a DSC7 Perkin-Elmer (Shelton, CT) apparatus at a scanning rate of 10°C/min, and using samples of ~10 mg. The melting temperature, T_f, was determined at the peak of the melting endotherm. The crystal weight fraction, W_c, was assessed from the melting enthalpy, assuming a value $\Delta H_f^\circ = 260$ J/g for the perfectly crystalline material.[7] The crystal volume fraction, ϕ_c, was computed from the crystal weight fraction, using $\rho_c = 1.49$ g/cm^3 and $\rho_a = 1.21$ g/cm^3 for the densities of the crystalline and amorphous components.[8]

TABLE I
Physical Characteristics of the Samples

Sample	W_c (%)	ρ[a] (g/cm^3)	ϕ_c (%)	$T_{\alpha\ \mathrm{peak}}$ (°C)	E' (GPa)
POM-N	87	1.45	83	—	—
POM-G	74	1.42	69	—	—
POM-NS	92	1.47	88	132	5.3 ± 0.2
POM-GS	86	1.45	82	128	4.5 ± 0.2
POM-CM	68	1.40	64	120	2.8 ± 0.1

W_c, crystal weight fraction; ρ, density; ϕ_c, crystal volume fraction; T_α, α relaxation peak temperature; E', storage modulus.
[a] Computed from the measured crystal weight fraction.

SAXS experiments were carried out in point focusing collimation, at room temperature, on the BM2-D2AM beam line of the European Synchrotron Radiation Facility (ESRF) in Grenoble, France, using an X-ray beam of wavelength $\lambda = 0.77$ Å (16 keV). The detector was a two-dimensional CCD camera from Roper Scientific. The patterns were corrected for the background scattering and for the geometry and intensity distortions of the CCD detector. The Lorentz-corrected intensity profiles from isotropic samples were plotted as a function of the wave vector, $q = 4\pi\sin\theta/\lambda$ with θ being one-half the scattering angle, after 360° azimuthal integration of the patterns. The most probable long period of the crystal-amorphous lamellar stacking, L_p, was determined from the maximum of the scattering peak using the Bragg relation

$$L_P = 2\pi/q_{\mathrm{peak}}. \tag{1}$$

The average crystal thickness, L_c, was computed from the relations $L_c = \phi_c L_p$, which assumes a much larger lateral extent of the crystalline lamellae as compared with their thickness.

Considering the Gibbs–Thomson equation[7]

$$T_f = T_f^0\left[1 - \frac{2\sigma_e}{(\rho_c \cdot L_c \cdot \Delta H_f^o)}\right], \tag{2}$$

where $T_f^\circ \approx 188$°C is the melting temperature of perfectly crystalline POM,[7] the determination of the actual melting temperature and crystal thickness of the materials gives access to the surface free energy, σ_e, of the folding surfaces of the crystallites.

SAXS experiments in the vicinity of the melting temperature have been carried out on a laboratory bench equipped with a CCD detector similar to the one used on the ESRF BM2-D2AM beam line. The Cu-K_α radiation was selected from a Rigaku rotating anode and collimated owing to a specific point-focusing Goebel mirror from Xenocs (Grenoble, France).

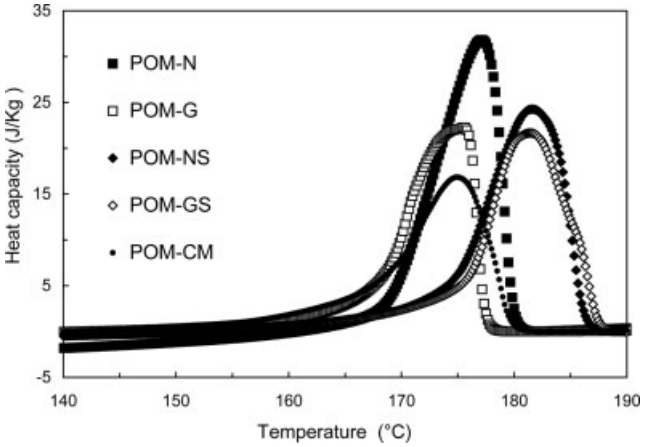

Figure 1 DSC heating curves of the various POM samples.

The samples were kept in a temperature-regulated oven equipped with Milar windows.

Dynamic mechanical analysis (DMA) has been conducted on a torsion pendulum as a function of temperature, at a frequency of 1 Hz and a heating rate of 1°C/min. The samples were strips 35 mm long, 2 mm wide, and 1 mm thick. The storage and loss modulus data were computed from integration of the stress and strain functions.

RESULTS AND DISCUSSION

Thermal behavior

The DSC heating curves displayed in Figure 1 show the melting endotherm of the crystalline phase of the sintered and compression-molded samples, together with that of the native and ground powders. The upward shift of the melting endotherm for the two sintered samples, as compared with their respective powders, is relevant to a structural reorganization within the crystalline phase during the sintering process. A priori, this increase in thermal stability is relevant to a significant thickening of the crystalline lamellae during the sintering process. However, in the case of semi-crystalline polymers that develop lamellar crystals, the Gibbs–Thomson relationship emphasizes the balanced roles of crystal thickness and surface free energy in the melting temperature variations, for a given polymer. The SAXS analysis in the next subsection will help clarify the situation in the present case.

The DSC melting curves of the POM-NS and POM-GS materials display a similitude which contrasts with the large difference between the melting curves of the two original powders (Fig. 1). This similitude of the two sintered materials reveals that the original crystalline phase of the powders is thoroughly reorganized during the sintering process, and the final morphology is very similar for the two sintered materials. As a corollary, it is suggested that a highly active molecular diffusion does occur within the crystalline phase at the sintering temperature.

Isothermal treatment for 30 min of a native powder in the DSC oven has been carried out to check the crucial role of the temperature during sintering. The DSC curves are reported in Figure 2. Starting from 150°C, the thermal treatment involves an upward shift of the melting endotherm and a concomitant increase of the melting peak temperature, till the temperature of 170°C. Beyond this temperature, both the melting temperature and crystallinity drop significantly. For a treatment temperature of 180°C, the melting endotherm is very similar to that of the compression-molded material. This means that, beyond the temperature of 170°C, which is the onset temperature of the melting endotherm of the native powder, major melting of the powder occurs during the 30-min isothermal treatment. This is evidence that the reorganization process giving rise to the melting temperature upward shift is a solid-state process that operates through molecular diffusion in the crystal, not in the melt.

Similar increased melting temperature due to crystal reorganization during annealing of various types of POM crystals has been reported by Jaffe and Wunderlich.[9] Former evidence of substantial crystal thickening by annealing in the temperature ranges between the crystalline relaxation and the melting temperature was reported for polyethylene.[10] The common structural feature between these highly crystalline polymers is the very high chain flexibility

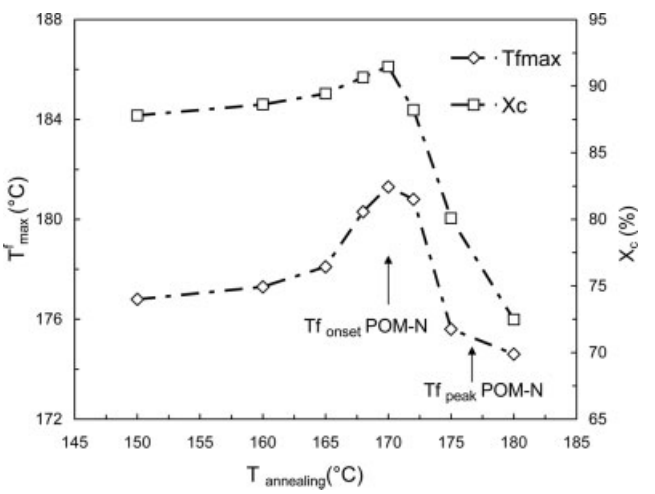

Figure 2 Plots of the melting temperature and weight fraction crystallinity of the POM-N powder samples after annealing for 30 min as a function of the annealing temperatures in the DSC oven (arrows indicate the melting onset and melting peak temperatures of the POM-N native powder before annealing).

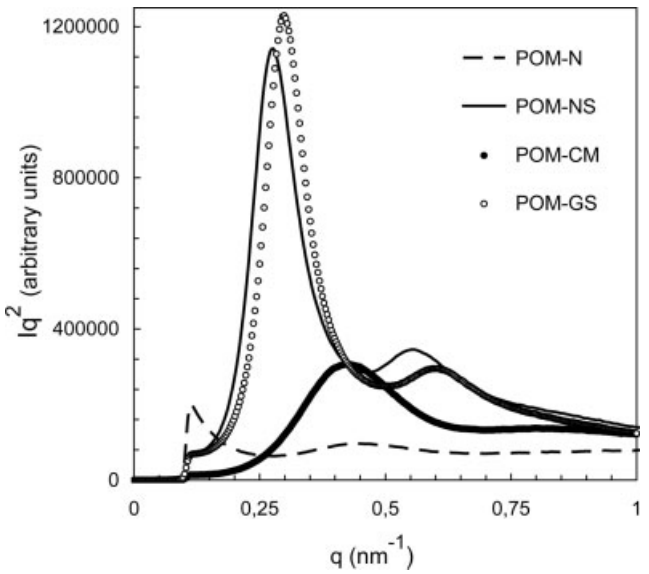

Figure 3 Lorentz-corrected SAXS intensity profiles of the POM-based materials at room temperature (ESRF experiments).

which enables a high-molecular mobility in the solid state.

SAXS characterization

Direct assessment of the crystal thickness has been carried by SAXS, for which the Lorentz-corrected SAXS profiles are reported in Figure 3. The POM-NS and the POM-GS display very similar SAXS profiles with a sharp correlation peak at very close scattering positions $q = 0.277$ nm^{-1} and $q = 0.298$ nm^{-1}, respectively. Besides, a very clear harmonic can be observed at a q-value about twice that of the main correlation peak, for both materials. This is relevant to a high degree of order of the lamella stacking that has been often observed in the case of highly crystalline polymers such as polyethylene.[10–12]

In contrast, the POM-N native powder and the POM-CM compression-molded materials do not display a scattering harmonic. The SAXS profile of the POM-G ground powder not shown in Figure 3 is very similar to that of POM-CM. The observation of a harmonic is a strong hint that the two sintered materials are much more regularly organized that their parent powders, as well as the material crystallized from the melt. Besides, as in the case of the melting behavior, the similitude of the SAXS profiles of POM-NS and POM-GS sintered materials gives evidence that the reorganization of the crystalline phase during sintering only depends on the processing treatment with no remaining signs of the initial crystalline morphology.

An analysis of an intercrystalline long period from the first correlation peak of the Lorentz-corrected intensity profiles has been performed owing to Bragg's relation. Table II reports the intercrystalline long period Lp, together with crystal and amorphous layers thicknesses, L_c and L_a, computed in consideration of the crystal volume fraction of the various samples. These data show that the crystalline lamellae of the sintered materials are much thicker than those of the corresponding powders, and the compression-molded material as well. This corroborates the previous conclusion of a reorganization in the crystalline phase toward greater perfection and greater thermal stability, during the sintering process. The increase of $\sim 70\%$ of the original crystal thickness is considerable in consideration of the 30-min duration of the 170°C treatment, during the sintering process. It emphasizes the high degree of molecular mobility in the crystalline phase at the temperature of the sintering process.

Using the crystal thickness data from SAXS in combination with the melting temperature and crystallinity data from DSC (Table II), the surface free energy of the crystallites has been computed for the various materials. The data presented in Table II show that surface free energy drops after the sintering operation: both POM-NS and POM-GS display σ_e data twice as low as their respective parent powders POM-N and POM-G. This is relevant to a significant ordering of the chain topology at the crystal surface during the thickening process. Indeed, according to previous studies on various types of polyethylene,[13,14] modifications of the chain-folded surface of the crystals should be accompanied by significant changes in the surface free energy, for instance a factor 2 has been reported between fringed-micelles and regular chain-folded crystals. Missing relevant data for POM, one may just suggest that chain folding is more regular in the sintered samples than in the parent powders. Worth noting is the comparison with a close parent, i.e., polyoxyethylene, for which a surface free energy range of 20–40 mJ/m^2 has been reported.[7] The fact that the present figures for the sintered samples are close to the lower bound of the surface energy range supports the above conclusion of regular chain-folding.

TABLE II
Structural Data for the Samples

Sample	L_p *(nm)*	L_c (nm)	L_a (nm)	$T_{f\ \mathrm{peak}}$ (°C)	σ_e (mJ/m^2)
POM-N	14.4	12.2	2.2	177.0	35
POM-G	14.8	10.6	4.2	175.5	34
POM-NS	22.8	20.1	2.7	181.5	16
POM-GS	21.0	17.2	3.8	181.5	14
POM-CM	15.0	9.4	5.6	175.0	37

L_p, most probable long period; L_c, crystal thickness; L_a, amorphous layer thickness; T_f, peak melting temperature; σ_e, surface free energy of the crystalline lamellae.

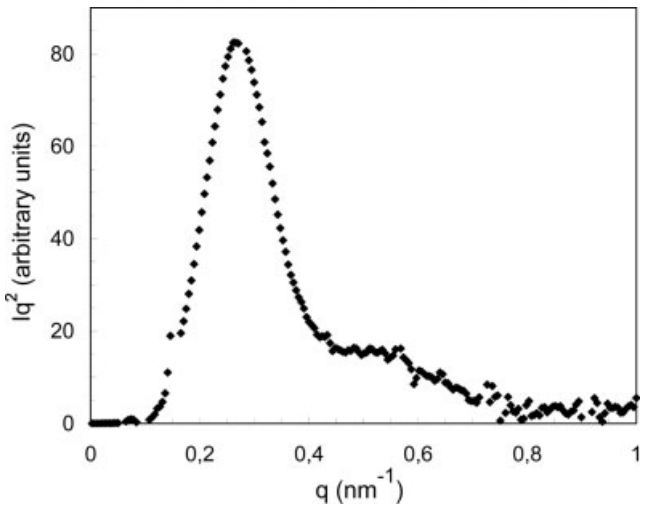

Figure 4 Lorentz-corrected SAXS intensity profile of POM-NS at 167°C (experiments on laboratory bench).

In contrast to our assignment of the double SAXS peaks to a harmonic phenomenon originating from a single well-ordered lamellar stacking, recent studies of nonisothermally crystallized POM materials reported the occurrence of double scattering peaks that were ascribed to two kinds of crystal populations: chain-extended and chain-folded crystals.[15,16] This interpretation relies on combined SAXS and Raman spectroscopic analyses, the latter method being able to identify the two species.[17] Actually, the so-called chain-extended crystals have been described as chain-folded crystals with taut tie chains in between due to secondary crystallization, which involves gradual stretching of the intercrystalline tie chains.[16] Notwithstanding this remark, the SAXS data of the present study do not support a double crystal population as can be judged from Figure 4, which shows the SAXS intensity profile of POM-NS recorded at 167°C, i.e., close to the melting temperature. These data reveal a uniform decrease of intensity of the coupled SAXS peaks, as compared with the same material at room temperature (Fig. 3). This is consistent with a partial melting of a single crystal population, as strongly suggested by the single melting peak in the DSC traces of POM-NS and POM-GS. Coexisting chain-folded and chain-extended crystals would have melted at different temperatures, involving a distinct disappearance of the two SAXS peaks. This finding supports the assignment of the second SAXS peak at a q-value that is twice that of the first one to a harmonic phenomenon (Fig. 3). This presence of a SAXS harmonic is also indicative of a highly regular stacking of lamellar crystals that is consistent with the above conclusion of a significant improvement of crystal perfection in POM-NS via crystal thickening and regular chain-folding.

Dynamic mechanical behavior

The storage modulus data of the sintered and the compression molded samples are reported in Table I. As already emphasized in the part I of this series,[6] the nearly 2-fold increase of POM-NS as compared with POM-CM is much more important than could be expected from the sole effect of the change in crystallinity. This can be ascribed to an increase in the crystal continuity that brings about mechanical percolation of the crystalline phase.

The loss modulus versus temperature plots for the sintered and compression-molded samples are shown in Figure 5. The low temperature relaxation associated with the glass transition of the amorphous phase of POM, at ~ -60°C, is barely affected by the processing. No significant change of the peak temperature of the relaxation can be observed. Only the amplitude of the relaxation displays a slight drop for the POM-NS. This may be mainly ascribed to the increase of crystallinity that reduces the amorphous phase contribution to the mechanical response.

In contrast, the high temperature relaxation associated with the activation of molecular mobility in the crystalline phase is sensitive to processing. The relaxation peak temperature slightly increases from 120°C for the POM-CM samples to 128°C and 132°C for the POM-GS and POM-NS, respectively (Table I). The temperature shift of the sintered material relaxation, in comparison with that of the compression-molded one, is a consequence of the crystal thickness increase. Several investigations on polyethylene have clearly demonstrated this relationship between crystal thickness and crystal relaxation temperature.[18,19] The reason lies in the thermal activation of the conformational defects which governs the relaxation process[20]: for a given frequency, i.e., for a given time, a higher temperature (i.e., a higher rate of displacement

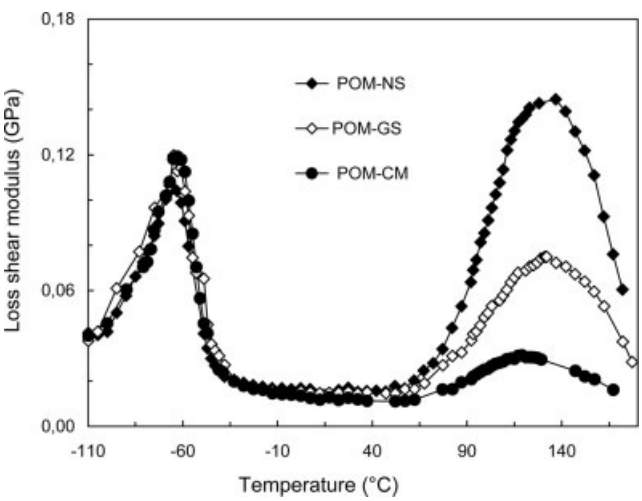

Figure 5 Loss modulus versus temperature for the various POM samples.

along the stems) is necessary for the defects to be able to cross a crystal lamella of larger thickness.

In parallel with the upward shit of the crystalline relaxation peak temperature, Figure 5 shows a change of the crystal damping capabilities in relation with processing: the POM-GS and POM-NS sintered materials exhibit respectively 2.5- and 5-fold increase of the relaxation amplitude as compared with the compression-molded sample. Considering the usual relaxation behavior of semi-crystalline polymers, this phenomenon mainly depends on crystallinity. However, as pointed out above regarding the storage modulus, the phenomenon is much more important than expected from the sole effect of the relative change of crystallinity, i.e., 25% and 33% increase for the POM-GS and POM-NS sintered materials as compared with the compression-molded sample (see Table I). Therefore, in agreement with our previous conclusion,[6] the present loss modulus data give evidence that the crystal phase undergoes a reorganization during sintering that improves its structural continuity and enhances its mechanical contribution, i.e., the damping behavior in the present instance.

Discussion of the sintering mechanism

Mechanical evaluation of bulk pieces sintered from POM powders, at various compaction temperatures, have shown that it is mandatory to reach the melting onset temperature range to get an efficient welding of the powder particles. The result is a 2-fold increase of the elastic modulus, as compared with the compression-molded material. Structural analyses have revealed that a reorganization in the crystalline phase, including crystal thickening and crystallinity increase, takes place during the sintering process. Annealing experiments carried out beyond the melting onset indicated that the partial melting of the powder should annihilate the sintering-induced crystalline reorganization, and thus the accompanying stiffness improvement. The substantial crystal thickening and crystallinity increase are strong indicators that molecular mobility is highly active at the sintering temperature of 170°C. This latter is indeed significantly higher than the peak temperature of the crystalline relaxation, i.e., 120°C and 132°C for the compression-molded and the material sintered from the native powder, respectively, at 1-Hz frequency. For instance, considering that the activation energy of a crystalline relaxation is ~100 kJ/mol, a rough estimation gives an activation frequency within the range of 10^4–10^5 Hz of the crystalline relaxation at 170°C. This figure supports the statement that sintering benefits from a highly active molecular mobility in the crystal.

The SEM shown in Figure 6 exhibits a strongly bounded powder particle in the sintered materials,

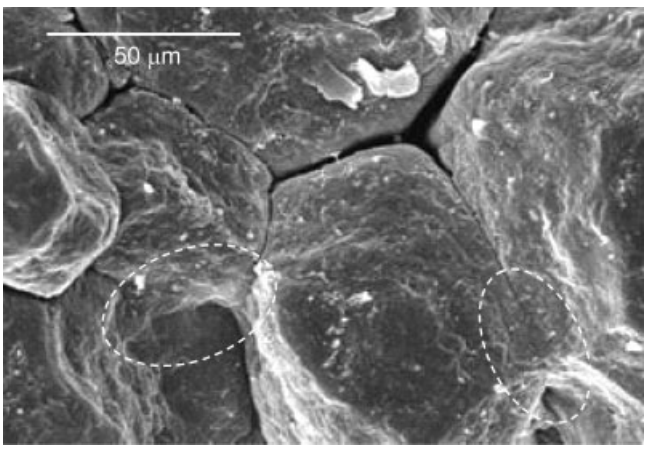

Figure 6 SEMs of a fracture surface of the POM-NS material.

providing evidence of intimate welding of the powder grains. One may see some particle with clear-cut transgranular fracture, which gives additional support to the strength of particle welding. Nevertheless, most of the fracture surface clearly results from interparticle crack propagation, with no signs of plastic deformation such as pull-out fibrils, indicating very limited molecular interpenetration through particle interfaces.

The first explanation that could be suggested for the efficient welding of the powder particles during sintering is the intertwining of chains over a limited depth through the surface of the contacting particles. As suggested in part I of this series,[6] such chain intertwining may occur in consideration that, at the processing temperature close to the melting onset, a very small amount of the most defective crystals is molten. The molten domains at the surface of adjacent particles can coalesce with chain-intertwining at the particle–particle interface, and then turn into interparticle crystalline bridges upon cooling. However, such events must be very scarce due to the faint amount of matter concerned. In addition, such melt-crystallized entities should generate pull-out fibrils at the particle interface after fracture. The missing of such fibrils in the SEM shown in Figure 6 supports the above assumption. Finally, data from Figure 2 predict that, in case of significant melting due to accidental temperature overshot beyond 170°C during the hot compaction process, a drop of both melting temperature and crystallinity would result. This is neither the case of POM-NS nor that of POM-GS.

In the case of no or very minor melting, intertwining of chains could be yet considered owing to the very active molecular mobility in the crystalline phase. The molecular mechanism of crystal thickening during annealing,[21] as sketched in Figure 7(a), is likely to favor molecular interpenetration over very limited depth at the contact surface of crystals from

adjacent particles via chain reptation through the intermediate amorphous layer in which chain entanglements are kept excluded from the crystal. Indeed, this latter process should be promoted by the migration of conformational defects such as chain jogs in the crystal,[8] as shown in Figure 7(b). This type of growth or plasticity defects[8,22] involves the switching of crystal stems in close-neighbor positions that increases the internal cohesion of the crystalline lamellae. It is worth noting that such a mechanism is unable to produce chain entanglements within the interlamellar amorphous regions, as would the melting of defective crystals discussed above.

In consideration of the above arguments, the buildup of particle connection during sintering is proposed to mainly operate via ''crystallographic welding'' of crystallites in close contact at the interface of adjacent particles. Owing to the conjunction of temperature and pressure, the plastic shear of the particles during sintering promotes the connection of close crystallites by matching crystallographic register into a monolithic crystal or as twinned crystals. The transformation of spherical particles of the native powder into polyhedral particle with not any remaining intergranular porosity in the POM-NS material (Fig. 6) gives evidence of an intense shear at the periphery of the particle, thanks to the compaction pressure largely exceeding the compressive yield stress.[6] The sketch displayed in Figure 8 features such a welding mechanism. The black stripes feature the chain stems within two crystalline lamellae of neighbor particles that build up crystallographic matching owing to temperature and shear, during the hot compaction process. For the sake of clarity, the crystallite and particle are not drawn at the same scale. Actually, the few tens of nanometers thick crystal lamellae are about four orders or magnitude smaller than the particles, so that tens of thousands of such crystallites can weld through the surfaces of every particle in the sintered materials. In this instance, the mechanism of chain diffusion

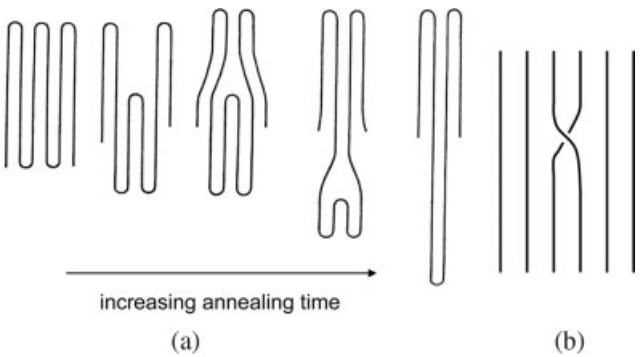

Figure 7 Schematic molecular models for (a) the mechanism of crystal thickening according to Wunderlich[21] and (b) a conformational jog defect resulting from thermodynamic disorder or plastic deformation.

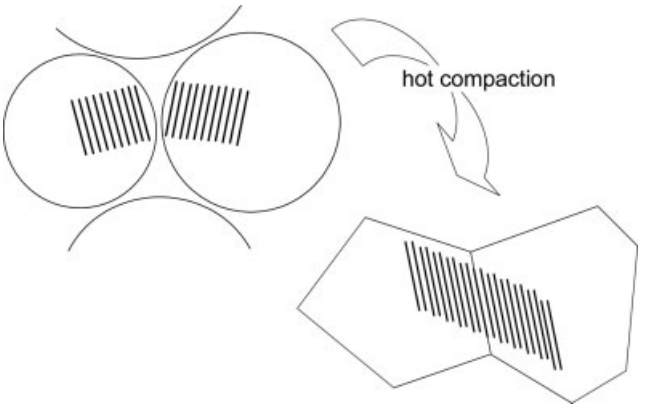

Figure 8 Structure model for the crystal welding at the particle interface during sintering (see text for details).

that is responsible for crystal thickening during sintering [Fig. 7(a)] should play a prime role in the welding efficiency, in combination with the shear stress, notably regarding the crystallographic matching of crystallites through the particle interface.

This structural model accounts for the enhanced structural continuity of the crystalline phase that has been concluded, on two occasions, in consideration of major sintering-induced mechanical effects: the very high stiffness of the materials in the temperature domain between the two mechanical relaxations and their damping behavior at the crystalline relaxation. The proposed model also accounts for mechanical behavior at rupture of the sintered materials. Indeed, in spite of the typically brittle behavior of these materials, their breaking stress exceeds the yield stress of the compression-molded materials. This is relevant to a particularly high resistance to plastic yielding of the crystalline phase which is consistent with the much larger crystal thickness of the sintered materials. The yield stress of semi-crystalline polymers is mainly governed by crystal thickness, as shown experimentally[23,24] and predicted theoretically.[25] Besides, the interparticle rupture of the sintered materials, without any signs of plastic deformation such as pull-out fibrils, is witnessing the lack of molecular intertwining at the particle interface. This topological deficiency makes the welded crystals of the sintered materials as brittle as chain-folded single crystals[26] or nonentangled low-molar-mass polymer crystals,[27,28] both of which break via crystal cleavage or splitting. However, in contrast to the above-mentioned systems, the high breaking stress of the sintered POM materials makes them perfectly able to undergo various types of machining.

CONCLUSION

Hot compaction of POM powders at temperature close to the melting onset, using pressure slightly higher

than the compressive yield stress at the same temperature, has been shown to enable efficient welding of the powder particles. Coherent bulk pieces were prepared, from which various types of samples could be obtained from by cutter-milling.[6] Comparison with compression-molded samples reveals a strong stiffness enhancement concomitant with a significant improvement of crystallinity. The detailed analysis of the mechanical behavior of the previous study and the damping behavior discussed in the present work indicates that a crystalline continuity builds up during sintering. Structural investigations corroborate the improvement of crystal organization, including crystal thickening.

The molecular mechanism of sintering is ascribed to the high-molecular mobility that allows both the crystal thickening and the welding of some crystals at the particle interface, in combination with the plastic shear of the particles. The resulting materials have very high stiffness and fairly high stress at break. Sintered materials are completely deprived of plastic capabilities due to missing chain intertwining at the particle interfaces, which prohibits the transmission of chain unfolding process throughout the sample beyond yielding. Notwithstanding, sintered materials can be easily machined out into samples of various shapes.

The authors are indebted to Dr. C. Chervin from Du Pont de Nemours, Geneva, Switzerland, for providing the POM powders.

References

1. Narkis, M. In Polymer Powder Technology, Narkis, M.; Rosenzweig, N., Eds.; Wiley: New York, 1995; Chapter 10.
2. Jog, P. J. Adv Polym Technol 1993, 12, 281.
3. Ariawan, A. B.; Ebnesajjad, S.; Hatzikiriakos, S. G. Powder Technol 2001, 121, 249.
4. Han, K. S.; Wallace, J. F.; Truss, R. W.; Geil, P. H. J Macromol Sci Phys 1981, B19, 313.
5. Zachariades, A. E. Polym Eng Sci 1985, 25, 747.
6. Al Jebawi, K.; Sixou, B.; Séguéla, R.; Vigier, G.; Chervin, C. J Appl Polym Sci 2006, 102, 1274.
7. Wunderlich, B. Macromolecular Physics; Vol 3: Crystal Melting; Academic Press: New York, 1980; Chapter 8.
8. Wunderlich, B. Macromolecular Physics; Vol 1: Crystal Structure, Morphology, Defects; Academic Press: New York, 1973; Chapter 4.
9. Jaffe, M.; Wunderlich, B. Kolloid-Z Z Polym 1967, 216, 203.
10. Statton, O. W.; Geil, P. H. J Appl Polym Sci 1960, 3, 357.
11. Reinhold, C.; Fischer, E. W.; Peterlin, A. J Appl Phys 1964, 35, 71.
12. Zhou, H.; Wilkes, G. L. Polymer 1997, 38, 5735.
13. Darras, O.; Séguéla, R. Polymer 1993, 34, 2946.
14. Bensason, S.; Minick, J.; Moet, A.; Chum, S.; Hiltner, A.; Baer, E. J Polym Sci Polym Phys 1996, 34, 1301.
15. Hama, H.; Tashiro, K. Polymer 2003, 44, 3107.
16. Hama, H.; Tashiro, K. Polymer 2003, 44, 2159.
17. Shimomura, M.; Igushi, M. Polymer 1982, 23, 509.
18. Takayanagi, M.; Matsuo, T. J Macromol Sci Phys 1967, 1, 771.
19. Popli, R.; Glotin, M.; Mandelkern, L.; Benson, R. S. J Polym Sci Polym Phys 1984, 22, 407.
20. Séguéla, R. J Polym Sci Polym Phys 2002, 40, 593.
21. Wunderlich, B. Macromolecular Physics; Vol 2: Crystal Nucleation, Growth, Annealing; Academic Press: New York, 1976; Chapter 7.
22. Schönherr, H.; Vancso, G. J.; Argon, A. S. Polymer 1995, 36, 2115.
23. Darras, O.; Séguéla, R. J Polym Sci Polym Phys 1993, 31, 759.
24. O'Kane, W. J.; Young, R. J. J Mater Sci Lett 1995, 14, 433.
25. Young, R. J. Philos Mag 1974, 30, 85.
26. Statton, O. W. J Appl Phys 1967, 38, 4149.
27. Peacock, A. J. Handbook of Polyethylene: Structures, Properties and Applications; Marcel Dekker: New York, 2000; Chapter 5.
28. Bessel, T. J.; Hull, D.; Shortall, J. B. J Mater Sci 1975, 10, 1127.